Shoot nitrate status regulates Arabidopsis shoot growth and systemic transcriptional responses via shoot adenylate isopentenyltransferase 3

Kota Monden[a†], Takamasa Suzuki[b], Mikiko Kojima[c], Yumiko Takebayashi[c], Daisuke Sugiura[d], Tsuyoshi Nakagawa[a], Hitoshi Sakakibara[c,d], and Takushi Hachiya[a†]

[a]Department of Molecular and Functional Genomics, Interdisciplinary Center for Science Research, Shimane University, 1060 Nishikawatsu-cho, Matsue, Shimane 690-8504, Japan

[b]College of Bioscience and Biotechnology, Chubu University, 1200 Matsumoto-cho, Kasugai, Aichi 487-8501, Japan

[c]RIKEN Center for Sustainable Resource Science, 1-7-22 Suehiro-cho, Tsurumi-ku, Yokohama, Kanagawa 230-0045, Japan

[d]Graduate School of Bioagricultural Sciences, Nagoya University, Furo-cho, Chikusa-ku, Nagoya, Aichi 464-8601, Japan

[†]Corresponding authors

Funding:

This study was supported by JSPS KAKENHI [No. 20K05771 and 23K04978 to TH and No. JP24KJ1709 to KM], by JST SPRING [No. JPMJSP2155 to KM], and by the Sasakawa Scientific Research Grant from the Japan Science Society [No. 2022-4039 to KM].

Keywords:

Arabidopsis thaliana; cytokinin; IPT3; isopentenyltransferase; micrografting; NR; nitrate reductase; nitrate signal; nitrogen satiety; systemic regulation

Summary Statement

Our novel experimental approach, combining micrografting and transfer experiments, reveals that shoot nitrate status regulates Arabidopsis shoot growth and systemic transcriptional responses via the shoot-expressed adenylate isopentenyltransferase 3

Abstract

Plants systemically regulate growth and gene expression according to their internal nitrate status. Our previous study reported that shoot nitrate accumulation increases shoot expression of *ADENYLATE ISOPENTENYLTRANSFERASE 3* (*IPT3*) and shoot levels of N^6-(Δ^2-isopentenyl) adenine (iP)-type cytokinin (CK). *IPT3* expression is localized in the phloem, and iP-type CKs, which are synthesized by IPT3, are phloem-mobile. Hence, systemic responses to shoot nitrate status may be regulated by the shoot-expressed IPT3. To examine this, we developed a novel system to manipulate nitrate levels and *IPT3* expression in a shoot-specific manner and performed growth analysis, CK determination, and RNA-sequencing. Our results demonstrated that shoot nitrate accumulation increased shoot growth and shoot concentrations of iP-type CKs via shoot IPT3. Transcriptomic responses to shoot nitrate satiety were largely tuned by shoot IPT3, with opposite effects in shoots and roots. Shoot IPT3 amplified shoot responses of nitrate-inducible genes and immune response genes to shoot nitrate accumulation, while dampened root responses of nitrate transport/assimilation genes. This transcriptomic modulation via shoot IPT3 was accompanied by coherent transcriptional changes in genes encoding mobile peptides and transcriptional repressors. Here we present a novel scheme integrating shoot nitrate satiety responses with CK signaling.

53 **Introduction**

54 Land plants use soil nitrate and ammonium as primary nitrogen sources. Nitrate serves as a
55 building block for organic nitrogen biosynthesis and as a signaling molecule (Remans et al. 2006;
56 Wang et al. 2004). The addition of exogenous nitrate to nitrate-depleted plants rapidly changes
57 the expression of nitrate-responsive genes, a phenomenon termed as the primary nitrate response
58 (PNR) (Medici and Krouk 2014). The nitrate transceptor nitrate transporter 1.1 (NRT1.1) and the
59 transcription-activating nitrate sensor NIN-like protein 7 (NLP7) play central roles in PNR
60 (Bouguyon et al. 2015; Ho et al. 2009; Liu et al. 2017; Liu et al. 2022). Nitrate uptake via NRT1.1
61 transiently elevates cytosolic and nuclear Ca^{2+} levels (Liu et al. 2017; Riveras et al. 2015; Wang
62 et al. 2021). The subgroup III calcium-dependent protein kinases 10/30/32 (CPK10/30/32)
63 perceive Ca^{2+} and phosphorylate NLP7 at S205, causing its nuclear retention. Nitrate-bound
64 NLP7 promotes the transcription of PNR genes, further altering expression of downstream genes.

65 Besides its role in PNR, nitrate acts as an internal signal of plant nitrogen status,
66 modulating nitrogen responses under steady-state conditions. In tobacco plants with different
67 nitrate reductase (NR) activities grown under varying nitrate availability, the shoot-to-root dry
68 weight ratio was positively correlated with foliar nitrate levels (Scheible et al. 1997). In
69 *Arabidopsis*, abundant nitrate application inhibits primary and lateral root growth (Patterson et al.
70 2016; Signora et al. 2001; Zhang et al. 1998). Patterson et al. (2016) reported that nitrate
71 application increases the shoot expression of glutaredoxin (Grx) genes *GrxS3/4/5/8* via
72 Arabidopsis response regulators (ARRs) 1/10/12 for cytokinin (CK) signaling, thereby inhibiting
73 primary root growth. Kobayashi et al. (2024) demonstrated that GrxS1–8 are phloem-mobile from
74 shoots to roots, and they bind to TGACG-binding factor 1 (TGA1) and TGA4 (Alvarez et al.
75 2014) in roots, forming a corepressor complex with TOPLESS to limit high-affinity nitrate uptake.
76 Meanwhile, Ota et al. (2020) discovered that under reduced shoot nitrogen, including nitrate
77 depletion, C-terminally encoded peptide downstream-like 2 (CEPDL2) is induced in the leaf
78 vasculature and subsequently translocated to the roots. The co-activator complex composed of

79 CEPDL2, its homologs CEPD1/2, and TGA1/4 promotes root nitrate uptake (Kobayashi et al.
80 2024). These findings imply that shoot nitrate status influences root nitrogen acquisition.
81 In our previous study, to focus on the action of shoot nitrate status, we manipulated
82 shoot nitrate levels using wild-type *Arabidopsis* and an NR-null mutant (Okamoto et al. 2019).
83 Subsequent RNA-sequencing (RNA-seq) suggested that shoot nitrate accumulation alone
84 represses the expression of nitrogen starvation-inducible genes in shoots and roots. Notably, we
85 observed that shoot nitrate accumulation was accompanied by increases in the shoot expression
86 of *ADENYLATE ISOPENTENYLTRANSFERASE 3* (*IPT3*) and the shoot levels of N^6-(Δ^2-
87 isopentenyl) adenine (iP)-type CK (Hachiya et al. 2020). *IPT3* expression is localized mainly in
88 phloem companion cells (Miyawaki et al. 2004; Takei et al. 2004a), and iP-type CKs, which are
89 de novo synthesized by IPT3, are phloem-mobile (Bishopp et al. 2011; Hirose et al. 2008). Hence,
90 systemic responses to shoot nitrate status may be regulated by IPT3-synthesized iP-type CKs.
91 Actually, nitrate- and CK-responsive genes have been found to partially overlap (Sakakibara et
92 al. 2006). Moreover, the nitrogen depletion-dependent induction of shoot *CEPDL2* is enhanced
93 by CKs translocated from roots (Ota et al. 2020). Furthermore, *trans*-zeatin (*t*Z)-type CKs mediate
94 preferential root growth in nitrate-rich patches over nitrate-poor patches (Poitout et al. 2018;
95 Ruffel et al. 2011). These features suggest systemic interplays between nitrogen and CK signaling.
96 Thus, the present study examined the systemic responses to shoot nitrate status and their
97 dependence on shoot IPT3. We developed a novel experimental system to manipulate nitrate
98 levels and *IPT3* expression in a shoot-specific manner using grafted plants derived from plants
99 lacking NR and/or IPT3. Using the shoots and roots of the grafted plants, growth analysis, CK
100 species determination, and RNA-seq were performed. Our results indicated that shoot nitrate
101 accumulation enhances shoot growth and alters the transcriptomes of shoots and roots, which is
102 elaborately tuned by shoot IPT3 in the opposite direction in shoots and roots. We herein present
103 a scheme incorporating shoot nitrate satiety responses with shoot IPT3 and iP-type CKs.
104

105 **Materials and Methods**

106 **Plant materials**

107 In this study, we used *A. thaliana* accession Columbia (Col) as the control line; NR-null (Wang
108 et al. 2007), *ipt3* (Miyawaki et al. 2006), and *ipt3,5,7* mutants (Miyawaki et al. 2006); and a
109 transgenic plant expressing *GFP* driven by the *IPT3* promoter (*proIPT3:GFP*) (Takei et al. 2004a).
110 Homozygous multiple mutants of NR-null *ipt3* and NR-null *proIPT3:GFP* were produced via
111 crossing.

112

113 **Culture media**

114 Three different solid media were used for *in vitro* plant culture as follows: (i) 2.5 mM NH_4^+
115 medium, half-strength Murashige and Skoog (1/2MS) modified basal salt mixture without
116 nitrogen (M531; PhytoTech Labs, Lenexa, KS, USA) supplemented with 1.25 mM $(NH_4)_2SO_4$,
117 10.0 g L^{-1} sucrose, 1.0 g L^{-1} MES, and 4.0 g L^{-1} gellan gum (Fujifilm Wako, Osaka, Japan) and
118 adjusted to pH 6.7 with KOH; (ii) 10 mM NO_3^- and 2.5 mM NH_4^+ medium, 1/2MS modified
119 basal salt mixture without nitrogen (M531; PhytoTech Labs) supplemented with 10 mM KNO_3,
120 1.25 mM $(NH_4)_2SO_4$, 10.0 g L^{-1} sucrose, 1.0 g L^{-1} MES, and 4.0 g L^{-1} gellan gum (Fujifilm
121 Wako) and adjusted to pH 6.7 with KOH; and (iii) no nitrogen medium, 1/2MS modified basal
122 salt mixture without nitrogen (M531; PhytoTech Labs) supplemented with 2.0 g L^{-1} sucrose, 0.5
123 g L^{-1} MES, and 5.0 g L^{-1} gellan gum (Fujifilm Wako) and adjusted to pH 5.7 with KOH.

124

125 **Transfer experiments using grafted plants**

126 Surface-sterilized seeds were placed in the dark at 4°C for 3 days to break seed dormancy. Then,
127 the seeds (approximately 120 seeds per dish) were sown in rectangle dishes (140 × 100 × 20 mm^3;
128 Eiken Chemical Co. Ltd., Tokyo, Japan) containing 50 mL of 2.5 mM NH_4^+ medium and grown
129 vertically at 22°C for 4 days under a photosynthetic photon flux density (PPFD) of 25 μmol m^{-2}
130 s^{-1} (16/8-h light/dark cycle). Four-day-old seedlings were micrografted aseptically in rectangle

131 dishes containing 50 mL of 2.5 mM NH_4^+ medium. The seedlings were cut perpendicularly in the
132 upper hypocotyl with an injection needle tip (NN-2613S; TERUMO, Tokyo, Japan) on a
133 membrane filter (HAWP04700; Merck Millipore, Darmstadt, Germany). The obtained scion was
134 connected with the partner rootstock through a 0.4-mm silicon microtube (1-8194-04; AS ONE,
135 Osaka, Japan). The grafted plants were incubated in a growth chamber at 27°C for 5 days under
136 a PPFD of 50 μmol m^{-2} s^{-1} (constant light) and further cultivated at 22°C for 24 h under a PPFD
137 of 25 μmol m^{-2} s^{-1} (16/8-h light/dark cycle). Successfully grafted plants without adventitious root
138 formation were selected for size uniformity. The grafted plants were transferred to round dishes
139 (diameter, 90 mm; depth, 20 mm; AS ONE) containing 30 mL of 10 mM NO_3^- and 2.5 mM NH_4^+
140 medium and grown for 24 h under a PPFD of 25 μmol m^{-2} s^{-1} (constant light). Finally, the plants
141 were transferred to round dishes containing 30 mL of no nitrogen medium and grown for 5 days
142 under a PPFD of 25 μmol m^{-2} s^{-1} (constant light). The surfaces of no nitrogen medium were
143 covered with cellophane sheets to allow nondestructive sampling of the roots (Hachiya et al.
144 2021a).
145
146 **Growth analysis**
147 Shoots and roots were weighed on a precision balance (HR-202i, A&D, Tokyo, Japan), and shoots
148 were scanned at a resolution of 600 dpi (GT-X980; EPSON, Tokyo, Japan) to measure the rosette
149 diameter. Leaf blades were harvested from the shoots and scanned at a resolution of 600 dpi to
150 measure the blade area of the cotyledon and true leaf. The rosette diameter and leaf blade area
151 were measured using ImageJ version 1.52p (US National Institutes of Health, Bethesda, MD,
152 USA).
153
154 **Determination of the total nitrogen content**
155 The total nitrogen concentration was quantified as previously described (Monden et al. 2022).
156 Harvested shoots and roots were oven-dried at 80°C for 2 days, and the dried samples were

157 ground using a spoon and stored in a desiccator before use. The dried powder was weighed and
158 encapsulated in a tin boat. Nitrogen concentrations were measured using a CN analyzer (Vario
159 EL III; Elementar Analysensysteme GmbH, Hanau, Germany).
160
161 **Determination of the nitrate content**
162 Nitrate content was quantified as previously described (Okamoto et al. 2019) with slight
163 modifications. Frozen samples were ground with a Multi-Beads Shocker (Yasui Kikai, Osaka,
164 Japan) using zirconia beads (diameter, 5 mm). The powder samples were boiled with 10 volumes
165 of Milli-Q water at 100°C for 20 min. Five microliters of the supernatant or 5 μL of standard
166 solution as dilution series of potassium nitrate was mixed with 40 μL of 0.05% (w/v) salicylic
167 acid in sulfuric acid. The resulting mixture was then incubated at room temperature for 20 min.
168 A mock treatment of 40 μL of sulfuric acid alone was added to 5 μL of the supernatant. One
169 microliter of 8% (w/v) NaOH solution was added to the mixture, and the nitrate content was
170 determined by measuring the absorbance at 410 nm using a plate reader (CORONA SH-9000Lab,
171 Hitachi High-Tech Corp., Tokyo, Japan).
172
173 **Observation of fluorescent signals**
174 Fluorescent imaging was performed using an All-in-one fluorescence microscope (BZ-X710,
175 KEYENCE, Osaka, Japan) with a 4× objective (CFI Plan Fluor DL 4×/0.13, Nikon, Tokyo, Japan)
176 and a metal halide lamp (No. 91056, KEYENCE). A narrow-band GFP filter (ex. 480/20; em.
177 510/20, 49020, Chroma, Brattleboro, VT, USA) and Cy5 filter (ex. 620/60; em. 700/75, 49006,
178 Chroma) were used to detect the fluorescence of GFP and chlorophyll, respectively.
179
180 **Determination of CK species**
181 The extraction and determination of CKs were performed as described previously (Kojima et al.
182 2009) using an ultra-performance liquid chromatography–tandem quadrupole mass spectrometry

183 system (AQUITY UPLC System/XEVO-TQS; Waters Corp., Milford, MA, USA) with an
184 octadecylsilyl column (ACQUITY UPLC HSS T3, 1.8 µm, 2.1 mm × 100 mm, Waters Corp.).
185
186 **Determination of the total protein content**
187 The total protein content was determined as previously described (Hachiya et al. 2016). Frozen
188 samples were ground with a Multi-Beads Shocker using zirconia beads (diameter, 5 mm). Total
189 proteins were extracted with 10 vol. of Laemmli buffer (2% (w/v) SDS, 62.5 mM Tris-HCl
190 (pH 6.8), 10% (v/v) glycerol, and 0.0125% (w/v) bromophenol blue) containing Halt™ protease
191 inhibitor cocktail (Thermo Fisher Scientific, Waltman, MA, USA), followed by incubation at
192 95°C for 5 min. Extracts were centrifuged at 20,400 × *g* at room temperature for 10 min, and 10
193 µL of each aliquot was suspended in 500 µL of deionized water. Next, 100 µL of 0.15% (w/v)
194 sodium deoxycholate was added, and the mixture was incubated at room temperature for 10 min.
195 One hundred microliters of 72% (v/v) trichloroacetic acid was added, followed by incubation at
196 room temperature for 15 min and centrifugation at 20,400 × *g* for 10 min. The precipitates were
197 air-dried and suspended in 25 µL of deionized water. The suspension was analyzed with a TaKaRa
198 BCA Protein Assay Kit (T9300A, TaKaRa, Kusatsu, Japan) according to the manufacturer's
199 instructions. Protein content was determined by measuring the absorbance at 562 nm using a plate
200 reader (Hitachi High-Tech Corp.)
201
202 **RNA extraction**
203 Frozen samples were ground with a Multi-Beads Shocker using zirconia beads (diameter, 5 mm).
204 Total RNA was extracted using an RNeasy Plant Mini Kit (Qiagen, Hilden, Germany) according
205 to the manufacturer's instructions. For RNA-seq library preparation, RNA was purified via on-
206 column DNase digestion (Qiagen).
207
208 **RNA-seq**

209 RNA quality was evaluated using a Qubit RNA IQ Assay Kit with a Qubit 4 Fluorometer (Thermo
210 Fisher Scientific). The RNA samples for which the RNA IQs ranged 9.4–10.0 were used for RNA-
211 seq. cDNA libraries were constructed using a NEBNext Ultra II RNA Library Prep with Sample
212 Purification Beads (E7775S, New England Biolabs, Ipswich, MA, USA), a NEBNext Poly(A)
213 mRNA Magnetic Isolation Module (E7490S, New England Biolabs), and a NEBNext Multiplex
214 Oligos for Illumina (E7710S, New England Biolabs) according to the manufacturer's instructions.
215 These cDNA libraries were sequenced using NextSeq 500 (Illumina, San Diego, CA, USA), and
216 the produced bcl files were converted to fastq files using bcl2fastq (Illumina). The reads were
217 analyzed according to a previously described method (Notaguchi et al. 2014) and mapped to the
218 Arabidopsis reference (TAIR10) using Bowtie (Langmead et al. 2009) with the following options:
219 "--all --best --strata." The mapped reads were processed using iDEP version 0.96 and 2.01 (Ge et
220 al. 2018). For data normalization, the read counts data were transformed with rlog and normalized
221 by subtracting the average expression for each gene according to the default setting of iDEP. For
222 DEG extraction, DESeq2 was run with a false-discovery rate cutoff of 0.1. The enrichment
223 analysis of each gene set was conducted using Metascape (Zhou et al. 2019) according to the
224 default setting.
225
226 **RT-qPCR**
227 Reverse transcription (RT) was performed using a ReverTraAce qPCR RT Master Mix with
228 gDNA Remover (Toyobo, Osaka Japan). RNA solution containing 0.5 μg of template RNA
229 served as the input. Synthesized cDNA was then diluted 5-fold with water and used for
230 quantitative PCR (qPCR). RT-qPCR was performed on a QuantStudio 1 (Thermo Fisher
231 Scientific) with KOD SYBR qPCR Mix (Toyobo). Relative transcript levels were calculated
232 using the comparative cycle threshold method, with *ACTIN3* as the internal standard (Hachiya et
233 al. 2021b). Primer sequences are presented in Table S1.
234

235 **Statistical analysis**

236 Unpaired two-tailed Welch's *t*-test and Tukey–Kramer multiple comparison test were performed
237 using R software v.2.15.3 (R Foundation for Statistical Computing, Vienna, Austria).

238

239 **Results and discussion**

240 **Manipulation of nitrate levels and *IPT3* expression in a shoot-specific manner**

241 To manipulate nitrate levels and *IPT3* expression in a shoot-specific manner, micrografting and
242 transfer experiments were performed using the wild-type (Col), NR-null mutant (NR-null, Wang
243 et al. 2007), *IPT3*-knockout mutant (*ipt3*, Miyawaki et al. 2006), NR-null *ipt3* mutant, and
244 *IPT3/IPT5/IPT7*-knockout mutant (*ipt3,5,7*, Miyawaki et al. 2006) (Figure 1A). The plants were
245 grown for 4 days in 2.5 mM NH_4^+ medium to ensure uniform growth regardless of the NR activity
246 (condition 1). Then, grafted plants corresponding to Col/*ipt3,5,7*, NR-null/*ipt3,5,7*, *ipt3*/*ipt3,5,7*,
247 and NR-null *ipt3*/*ipt3,5,7* (scion line name/rootstock line name) were generated (Figure S1A;
248 conditions 2 and 3). Notably, *ipt3,5,7* was used as the rootstock to avoid the complementation of
249 shoot-specific CK depletion in *ipt3* by root-derived CKs. RT-PCR with primers specific for *NIA1*,
250 *NIA2*, *IPT3*, *IPT5*, *IPT7*, and *ACTIN2* confirmed the successful generation of the desired grafted
251 plants (Figure S1B). The grafted plants were transferred to 10 mM NO_3^- and 2.5 mM NH_4^+
252 medium and incubated for 24 h to allow nitrate accumulation (condition 4). Then, the plants were
253 transferred to no nitrogen medium and grown for 5 days (condition 5). After nitrogen removal,
254 nitrate concentrations generally decreased over time in the shoots and roots of all plants (Figure
255 1B, C). At 3 and 5 days after nitrogen removal, the shoot nitrate concentrations were higher in
256 NR-null/*ipt3,5,7* and NR-null *ipt3*/*ipt3,5,7* plants than in the other plants (Figure 1B), whereas
257 root nitrate was depleted to the same level in all plants (Figure 1C). Meanwhile, at 5 days after
258 nitrogen removal, total protein and total nitrogen levels in shoots and roots differed little among
259 the plants (Figure 1D–G). RT-qPCR revealed that shoot *IPT3* expression was significantly higher
260 in NR-null/*ipt3,5,7* than in Col/*ipt3,5,7* (Figure 1H). To visualize the tissue-specific induction of

261 *IPT3* as a result of shoot NR deficiency, scions from *proIPT3:GFP* and NR-null *proIPT3:GFP*
262 plants were grafted onto *ipt3,5,7* rootstocks, followed by the same transfer experiment as before.
263 Shoot nitrate accumulation and *GFP* induction were observed in NR-null *proIPT3:GFP*/*ipt3,5,7*
264 plants 5 days after nitrogen removal (Figure 1I, J), with strong GFP fluorescence localized in the
265 leaf vein (Figure 1K). These findings suggest that *IPT3* induction due to shoot nitrate satiety
266 occurs mainly in the vasculature. Overall, we successfully developed a novel system that
267 manipulates nitrate levels and *IPT3* expression in a shoot-specific manner, with minimal impact
268 on the total protein and total nitrogen levels within the plant, in the absence of external nitrogen
269 sources. This system allows the analysis of systemic responses to shoot nitrate status and their
270 dependence on shoot IPT3 in the following experiments.
271
272 **Shoot nitrate satiety elevates shoot levels of iP-type CKs via shoot IPT3**
273 To assess the impact of shoot nitrate status and shoot *IPT3* expression on CK activity, we
274 measured the concentrations of iP-type and *t*Z-type CKs. The experiments were performed using
275 the shoots and roots of grafted plants, with three biological replicates collected independently
276 (Figure 2) or simultaneously (Figure S2). The levels of iP ribotides (iPRPs), iP-7-*N*-glucoside
277 (iP7G), iP-9-*N*-glucoside (iP9G), *t*Z ribotides (*t*ZRPs), *t*Z-7-*N*-glucoside (*t*Z7G), *t*Z-9-*N*-
278 glucoside (*t*Z9G), *t*Z-*O*-glucoside (*t*ZOG), and *t*ZR-*O*-glucoside (*t*ZROG) were consistently
279 lower in the shoots of *ipt3*/*ipt3,5,7* and NR-null *ipt3*/*ipt3,5,7* plants than in those of Col/*ipt3,5,7*
280 and NR-null/*ipt3,5,7* plants (Figure 2C–E, 2H–L and Figure S2C–E, S2H–L). Meanwhile, little
281 difference was observed in the root levels of CK species among the grafted plants. These
282 observations indicated that shoot IPT3 is crucial for maintaining the shoot levels of *t*Z-type and
283 iP-type CKs, but it has only a minor effect on root CK levels. Notably, the shoot levels of iPRPs,
284 iP7G, and iP9G were significantly increased by shoot NR deficiency in the presence of shoot
285 IPT3 but not in its absence (Figure 2C–E and Figure S2C–E). This finding suggests that shoot
286 nitrate satiety elevates the shoot levels of iP-type CKs via shoot IPT3.

287

288 **Shoot nitrate satiety enhances shoot growth via shoot IPT3**

289 To determine the effects of shoot nitrate status and shoot *IPT3* expression on plant growth, we
290 analyzed growth parameters using all grafted plants from five independent experiments (Figure
291 3). Shoot fresh weight, leaf blade area, rosette diameter, and leaf number were significantly lower
292 in *ipt3*/*ipt3,5,7* and NR-null *ipt3*/*ipt3,5,7* plants than in Col/*ipt3,5,7* and NR-null/*ipt3,5,7* plants
293 (Figure 3B–E). Meanwhile, no significant difference was observed in the root fresh weight among
294 the grafted plants (Figure 3F). These observations indicate that shoot IPT3 generally contributes
295 to shoot growth. Importantly, shoot appearance, shoot fresh weight, and leaf blade area were
296 significantly increased by shoot NR deficiency in the presence of shoot IPT3 but not in its absence
297 (Figure 3A–C). A similar trend was observed for the rosette diameter, although the differences
298 were not statistically significant (Figure 3D). These patterns correspond to the findings for shoot
299 iPRP, iP7G, and iP9G concentrations (Figure 2C–E and Figure S2C–E). Actually, shoot fresh
300 weight and leaf blade area were strongly correlated with levels of these iP-type CKs (Figure S3).
301 Overall, these findings suggest that shoot nitrate satiety promotes shoot growth by increasing
302 IPT3 and iP-type CK biosynthesis in the shoot. It is well established that in Arabidopsis plants,
303 root-supplied nitrate stimulates the biosynthesis of *t*Z-type CKs in the root and facilitates their
304 transport to the shoot, thereby promoting shoot growth (Kiba et al. 2013; Osugi et al. 2017;
305 Sakakibara, 2021). Collectively, shoot-derived iP-type CKs and root-derived *t*Z-type CKs may
306 regulate shoot growth by responding to the internal and external nitrate status, respectively.

307

308 **Transcriptomic responses to shoot nitrate satiety are tuned via shoot IPT3 with opposite**
309 **effects in shoots and roots**

310 To investigate the effects of shoot nitrate status and shoot *IPT3* expression on systemic responses,
311 we performed RNA-seq using the shoots and roots of grafted plants, with three biological
312 replicates collected independently. Reads per million mapped reads (RPM; Table S2) and

313 normalized transcript levels (Table S3) were calculated according to the read counts. To identify
314 genes regulated by shoot nitrate accumulation and further modulated by shoot IPT3, we extracted
315 differentially expressed genes (DEGs) between NR-null/*ipt3,5,7* and Col/*ipt3,5,7* and between
316 NR-null *ipt3*/*ipt3,5,7* and *ipt3*/*ipt3,5,7* with a minimum fold change of 1.5 (Figure 4A and Figure
317 S4 and Table S4). Comparison of these DEGs between shoots and roots revealed minimal overlap
318 (Figure S4), indicating that shoots and roots express distinct sets of genes regulated by shoot
319 nitrate accumulation. Hence, we analyzed the shoot and root transcriptomes separately. In shoots,
320 the number of DEGs was larger between NR-null/*ipt3,5,7* and Col/*ipt3,5,7* than between NR-null
321 *ipt3*/*ipt3,5,7* and *ipt3*/*ipt3,5,7* (Figure 4A). Thus, 631 DEGs were identified as candidate genes
322 upregulated by shoot nitrate accumulation, with their responses enhanced by shoot IPT3.
323 Meanwhile, 663 DEGs were candidates downregulated by shoot nitrate accumulation, with their
324 responses enhanced by shoot IPT3. By contrast, in roots, the number of DEGs was lower between
325 NR-null/*ipt3,5,7* and Col/*ipt3,5,7* than between NR-null *ipt3*/*ipt3,5,7* and *ipt3*/*ipt3,5,7* (Figure
326 4A). Thus, 189 DEGs were identified as candidate genes upregulated by shoot nitrate
327 accumulation, with their responses dampened by shoot IPT3, whereas 126 DEGs were candidates
328 downregulated by shoot nitrate accumulation, with their responses dampened by shoot IPT3.
329 Correspondingly, the shoot transcriptional responses of 631 and 663 DEGs to shoot NR
330 deficiency were decreased by shoot IPT3 deficiency (Figure 4B, C), whereas the root responses
331 of 189 and 126 DEGs were augmented by shoot IPT3 deficiency (Figure 4D, E). Three
332 independent RNA-seq results exhibited similar trends; therefore, only the mean transcript levels
333 are presented in subsequent figures for clarity, unless otherwise stated. k-means clustering
334 identified 11 clusters in which gene expression was significantly altered by shoot NR deficiency,
335 with their responses modulated by shoot IPT3 deficiency in the opposite direction in shoots and
336 roots (Figure S5, S6 and Table S5). In summary, shoot transcriptional responses to shoot nitrate
337 satiety are generally enhanced by shoot IPT3, whereas root responses are dampened by shoot
338 IPT3.

339 Enrichment analyses of the 11 clusters from Figure S5 and S6 revealed a diverse set
340 of genes significantly regulated by shoot nitrate and shoot IPT3. In shoots, the cluster 6 and 8
341 enriched terms related to translation, primary carbon metabolism, and biotic stress response such
342 as "ath03010: Ribosome", "WP2621: Glycolysis", and "GO:0009617: response to bacterium"
343 (Figure S5A). Previously, we reported that shoot nitrate accumulation is accompanied by the
344 upregulation of ribosome-associated genes in shoots (Hachiya et al. 2020). It is widely known
345 that cytokinin signal upregulates genes encoding ribosomal proteins and elongation factors
346 (Sakakibara et al. 2006). Hence, translation may be activated by shoot nitrate satiety, some of
347 which are mediated by shoot IPT3 (Figure S5B). Meanwhile, terms related to wounding and
348 jasmonic acids were overrepresented in both cluster 3 and 7 (Figure S5A). Thus, stress responses
349 associated with jasmonic acids signaling could be downregulated by shoot nitrate satiety, which
350 is enhanced by shoot IPT3 (Figure S5B). In roots, the cluster 11, 12, and 14 predominantly
351 featured terms related to abiotic and biotic stresses, particularly hypoxia (Figure S6A). The cluster
352 15 and 16 enriched terms associated with translation, biosynthesis, and nitrate transport (Figure
353 S6A). Notably, the genes encoding nitrate reductases (NIA1, NIA2) and high-affinity nitrate
354 transporters (NRT2.1, NRT2.4, NRT2.5, NRT3.1) were included in the cluster 16 (Table S5).
355 Thus, shoot nitrate satiety suppresses anabolism including nitrogen assimilation in the roots, the
356 responses of which are dampened by shoot IPT3 (Figure S6B).
357
358 **Shoot nitrate satiety induces shoot *ARR2* expression via shoot IPT3**
359 We examined the shoot expression of CK-inducible genes using a shared list across multiple
360 studies (Bhargava et al. 2013). However, our survey failed to detect their transcriptional changes
361 associated with shoot NR and/or IPT3 deficiency (Figure S7A and Table S6). Notably, previous
362 studies analyzed early transcriptomic responses to exogenous application of *t*Z and benzyladenine
363 (Bhargava et al. 2013); therefore, conventional gene lists might be unsuitable for evaluating
364 steady-state responses to alterations of endogenous iP-type CKs. Our meticulous investigation

365 discovered that shoot expression of the type-B response regulator gene *ARR2* was induced by
366 shoot NR deficiency in the presence of shoot IPT3 but not in its absence (Figure S7B), a finding
367 corroborated by RT-qPCR (Figure S7C). Choi et al. (2010) demonstrated that CK-activated
368 ARR2 enhances Arabidopsis immunity through direct binding with the transcription factor TGA3.
369 In Figure S5A, the cluster 8 derived from clustering was overrepresented in terms such as
370 "GO:0009617: response to bacterium" and "GO:0009627: systemic acquired resistance" (Figure
371 S5A). Thus, shoot nitrate satiety might enhance immunity by upregulating *ARR2* via shoot IPT3.
372 Furthermore, given that *ARR2*-overexpressing plants exhibit larger rosette leaves and biomass
373 (Arnaud et al. 2017), it is plausible that shoot nitrate satiety could promote shoot growth partly
374 via shoot IPT3–ARR2 cascade.
375
376 **Transcriptional responses of nitrate–CPKs–NLPs-regulatory genes to shoot nitrate satiety**
377 **are enhanced via shoot IPT3**
378 Previously, we reported that the expression of nitrate-responsive genes is influenced by shoot
379 nitrate accumulation (Okamoto et al. 2019), prompting our focus on these genes. In shoots, the
380 transcript levels of genes induced by nitrate itself (Wang et al. 2004) were significantly increased
381 by shoot NR deficiency, and this induction was attenuated by shoot IPT3 deficiency (Figure 5A
382 and Table S7). By contrast, there was minimal variation in the root expression of nitrate-inducible
383 genes among the plants. Given that CPK10/30/32, NLP7, and its homologs (NLPs) govern nitrate-
384 dependent gene expression (Liu et al. 2017; Liu et al. 2022), we analyzed the expression of genes
385 induced by nitrate–CPKs–NLPs signaling. In shoots, the genes induced via CPK10/30/32 and
386 those co-induced via all NLPs exhibited similar expression patterns as the nitrate-inducible genes
387 (Figure 5A–C and Table S7). Meanwhile, none of the genes induced exclusively by individual
388 NLPs exhibited different expression patterns among the plants (Figure S8 and Table S8). In roots,
389 the expression of genes regulated via CPK10/30/32 and NLPs showed little variation among the
390 plants (Figure 5B, C and Figure S8 and Table S7, S8). These findings suggest that shoot nitrate

391 satiety upregulates nitrate-inducible genes via CPK10/30/32 and multiple NLPs specifically in
392 the shoots, with their responses enhanced by shoot IPT3.
393
394 **Transcriptional responses of nitrogen starvation-inducible genes to shoot nitrate satiety are**
395 **tuned via shoot IPT3 in the opposite direction in shoots and roots**
396 Previously, we reported that shoot nitrate accumulation alleviates nitrogen starvation responses
397 (Okamoto et al. 2019). Thus, we analyzed the responses of two independent sets of nitrogen
398 starvation-inducible gene (Kiba et al. 2018; Krapp et al. 2011). Although these gene sets are quite
399 distinct (Figure S9A), shoot NR deficiency consistently repressed shoot expression of nitrogen
400 starvation-inducible genes, with this repression slightly alleviated by shoot IPT3 deficiency
401 (Figure S9B, C). The nitrogen starvation-inducible genes common to both gene sets exhibited a
402 similar but stronger tendency (Figure 5D). Meanwhile, the root expression of nitrogen starvation
403 inducible-genes were significantly repressed by shoot NR deficiency only in the absence of shoot
404 IPT3 (Figure 5D and S9B, C). Overall, the repression of nitrogen starvation-inducible genes to
405 shoot nitrate satiety is enhanced by shoot IPT3 in the shoot, but dampened in the root.
406 Several genes involved in nitrogen transport and assimilation in the root are often
407 induced under nitrogen starvation (Kiba et al. 2018; Krapp et al. 2011), and thus, we focused on
408 their root expression. Most of the genes involved in high-affinity nitrate transport and nitrogen
409 assimilation were slightly downregulated by shoot NR deficiency, and these responses were
410 remarkably intensified by shoot IPT3 deficiency (Figure 5E). Thus, the degree of downregulation
411 in root nitrate utilization due to shoot nitrate satiety is largely dependent on shoot IPT3. By
412 contrast, genes involved in dual-affinity/low-affinity nitrate transport (*NRT1.1* and *NRT1.2*) (Liu
413 et al. 1999) were upregulated by shoot NR deficiency regardless of the presence of shoot IPT3
414 (Figure 5E). Because NRT1.1 and NRT1.2 can facilitate the uptake of auxin and abscisic acid,
415 respectively (Kanno et al. 2012; Krouk et al. 2010), their upregulation may not necessarily be
416 related to nitrate acquisition.

417

418 **Systemic regulation of nitrogen starvation-inducible genes regulated by shoot nitrate satiety**
419 **may be mediated via transcriptional repressors and mobile peptides**

420 Nitrate signaling induces nitrate-inducible GARP-type transcriptional repressor 1 clade genes
421 (*NIGT1.1/1.2/1.3/1.4*) and *LOB DOMAIN-CONTAINING PROTEIN 37/38/39* genes
422 (*LBD37/38/39*) via NLPs (Kiba et al. 2018; Maeda et al. 2018; Marchive et al. 2013; Rubin et al.
423 2009; Safi et al 2021). These translational products act as repressors to downregulate nitrogen
424 starvation-inducible genes. Thus, we examined these repressor genes. In the shoot, the transcript
425 levels of *NIGT1.1* and *LBD37* were increased by shoot NR deficiency, and this induction were
426 attenuated by shoot IPT deficiency (Figure 5F). The expression of these repressors exhibited a
427 strong negative correlation with nitrogen starvation-inducible genes (Figure S10). In the root, the
428 transcript levels of *NIGT1.1/1.2* and *LBD37/38* were increased by shoot NR deficiency, and this
429 induction was enhanced by shoot IPT3 deficiency (Figure 5G). These repressors also showed a
430 strong negative correlation with nitrogen starvation-inducible genes (Figure S10). These findings
431 suggest that shoot nitrate satiety and shoot IPT3 regulate the systemic regulation of nitrogen
432 starvation-inducible genes via these repressors. It is valuable to explore whether iP-type CKs
433 synthesized by shoot IPT3 systemically regulate the root expression of repressor genes.

434 Next, we focused on shoot-to-root mobile peptides regulating systemic nitrogen
435 starvation responses, i.e., CEPD1/2, CEPDL2, and GrxS1–8 (Kobayashi et al. 2024; Ohkubo et
436 al. 2017; Ota et al. 2020) (Figure 5H and S11). The co-activator complexes composed of
437 CEPD1/2/CEPDL2 and TGA1/4 promote root nitrate uptake via upregulation of *NRT2.1* and
438 *CEPH*, whereas the co-repressor complexes of GrxS1–8 and TGA1/4 repress it (Kobayashi et al.
439 2024). The root expression of *NRT2.1* and *CEPH* was positively correlated with shoot expression
440 of *CEPDL2*, whereas negatively correlated with shoot expression of *GrxS3* and *GrxS5* (Figure
441 5H and S11). These findings suggest that shoot nitrate satiety and shoot IPT3 regulate the
442 systemic regulation of root nitrate uptake via shoot-to-root mobile peptides.

443

444 **Conclusion: a scheme integrating shoot nitrate satiety responses with shoot IPT3**

445 Our experimental system elucidated the systemic responses to shoot nitrate status and their
446 dependence on shoot IPT3, although primary and secondary responses remain indistinguishable.
447 A novel scheme for the systemic responses is summarized in Figure 6: shoot nitrate satiety
448 enhances shoot growth and the shoot expression of *IPT3*, nitrate–CPKs–NLPs-inducible genes
449 including nitrate uptake/assimilation genes, and immune response genes, with their responses
450 enhanced by shoot IPT3. Meanwhile, shoot nitrate satiety decreases the root expression of
451 nitrogen starvation-inducible genes and nitrate uptake/assimilation genes, with their responses
452 dampened by shoot IPT3. Hence, under shoot nitrate satiety, shoot IPT3 would promote nitrogen
453 utilization at the whole-plant scale, providing organic nitrogen crucial for shoot growth
454 enhancement. Notably, plant CK levels are generally reduced by prolonged abiotic stresses
455 including salinity, drought, chilling, and heat (Cortleven et al. 2019), during which shoot growth
456 is usually suppressed. Thus, shoot growth and nitrogen utilization, which are tuned by shoot IPT3
457 depending on shoot nitrate status, would be further fine-tuned via modulation of CK levels
458 depending on abiotic stresses. Such crosstalk in CK signaling would optimize plant growth and
459 nitrogen utilization in fluctuating environments.

460

461 **Acknowledgements**

462 The NR-null seeds were kindly provided by Dr. Nigel M. Crawford (University of California,
463 San Diego). The *ipt3* and *ipt3,5,7* seeds were kindly provided by Dr. Tatsuo Kakimoto (Osaka
464 University). We thank Ms. Yuki Okamoto and Mr. Masahiro Watanabe for their support in the
465 preparation of the plant materials. This study was supported by JSPS KAKENHI [No. 20K05771
466 and 23K04978 to TH and No. JP24KJ1709 to KM], by JST SPRING [No. JPMJSP2155 to KM],
467 and by the Sasakawa Scientific Research Grant from the Japan Science Society [No. 2022-4039
468 to KM].

469

470 **Conflicts of interest**

471 The authors declare no competing interests.

472

473 **Data Availability Statement**

474 The RNA-seq raw data are available in ArrayExpress under the accession number E-MTAB-
475 14302 (https://www.ebi.ac.uk/biostudies/arrayexpress).

476

477 **References**

478 Alvarez, J. M., E. Riveras, E. A. Vidal, et al. 2014. "Systems approach identifies TGA1 and TGA4
479 transcription factors as important regulatory components of the nitrate response of *Arabidopsis*
480 *thaliana* roots." *The Plant Journal* 80, no. 1: 1–13. https://doi.org/10.1111/tpj.12618.

481

482 Arnaud, D., S. Lee, Y. Takebayashi, D. Choi, J. Choi, H. Sakakibara, and I. Hwang. 2017.
483 "Cytokinin-mediated regulation of reactive oxygen species homeostasis modulates stomatal
484 immunity in Arabidopsis." *The Plant Cell* 29, no. 3: 543–559.
485 https://doi.org/10.1105/tpc.16.00583.

486

487 Bishopp, A., S. Lehesranta, A. Vatén, S. El-Showk, B. Scheres, K. Helariutta, A. P. Mähönen, H.
488 Sakakibara, and Y. Helariutta. 2011. "Phloem-transported cytokinin regulates polar auxin
489 transport and maintains vascular pattern in the root meristem." *Current Biology* 21, no. 11: 927–
490 932. https://doi.org/10.1016/j.cub.2011.04.049.

491

492 Bouguyon, E., F. Brun, D. Meynard, et al. 2015. "Multiple mechanisms of nitrate sensing by
493 *Arabidopsis* nitrate transceptor NRT1.1." *Nature Plants* 1: 15015.

494 https://doi.org/10.1038/nplants.2015.15.

495

496 Choi, J., S. U. Huh, M. Kojima, H. Sakakibara, K. H. Paek, and I. Hwang. 2010. "The cytokinin-
497 activated transcription factor ARR2 promotes plant immunity via TGA3/NPR1-dependent
498 salicylic acid signaling in *Arabidopsis*." *Developmental Cell* 19, no. 2: 284–295.
499 https://doi.org/10.1016/j.devcel.2010.07.011.

500

501 Cortleven, A., J. E. Leuendorf, M. Frank, D. Pezzetta, S. Bolt, and T. Schmülling. 2019.
502 "Cytokinin action in response to abiotic and biotic stresses in plants." *Plant, Cell & Environment*
503 42, no. 3: 998–1018. https://doi.org/10.1111/pce.13494.

504

505 Ge, S. X., E. W. Son, and R. Yao. 2018. "iDEP: an integrated web application for differential
506 expression and pathway analysis of RNA-Seq data." *BMC Bioinformatics* 19: 534.
507 https://doi.org/10.1186/s12859-018-2486-6.

508

509 Hachiya, T., N. Ueda, M. Kitagawa, G. Hanke, A. Suzuki, T. Hase, and H. Sakakibara. 2016.
510 "Arabidopsis root-type ferredoxin:NADP(H) oxidoreductase 2 is involved in detoxification of
511 nitrite in roots." *Plant and Cell Physiology* 57, no. 11: 2440–2450.
512 https://doi.org/10.1093/pcp/pcw158.

513

514 Hachiya, T., Y. Okamoto, M. Watanabe, Y. Takebayashi, M. Kojima, T. Suzuki, and H.
515 Sakakibara. 2020. "Genome-wide responses to shoot nitrate satiety are attenuated by external
516 ammonium in *Arabidopsis thaliana*." *Soil Science and Plant Nutrition* 66, no. 2: 317–327.
517 https://doi.org/10.1080/00380768.2020.1717905.

518

519 Hachiya, T., T. Oya, K. Monden, A. Nagae, and T. Nakagawa. 2021a. "A cellophane-supported

520 *Arabidopsis* culture for seamless transfer between different media is useful for studying various
521 nitrogen responses." *Soil Science and Plant Nutrition* 67, no. 3: 277–282.
522 https://doi.org/10.1080/00380768.2021.1908094.
523
524 Hachiya, T., J. Inaba, M. Wakazaki, et al. 2021b. "Excessive ammonium assimilation by plastidic
525 glutamine synthetase causes ammonium toxicity in *Arabidopsis thaliana*." *Nature*
526 *Communications* 12: 4944. https://doi.org/10.1038/s41467-021-25238-7.
527
528 Hirose, N., K. Takei, T. Kuroha, T. Kamada-Nobusada, H. Hayashi, and H. Sakakibara. 2008.
529 "Regulation of cytokinin biosynthesis, compartmentalization and translocation." *Journal of*
530 *Experimental Botany* 59, no. 1: 75–83. https://doi.org/10.1093/jxb/erm157.
531
532 Ho, C. H., S. H. Lin, H. C. Hu, and Y. F. Tsay. 2009. "CHL1 functions as a nitrate sensor in
533 plants." *Cell* 138, no. 6: 1184–1194. https://doi.org/10.1016/j.cell.2009.07.004.
534
535 Kanno, Y., A. Hanada, Y. Chiba, T. Ichikawa, M. Nakazawa, M. Matsui, T. Koshiba, Y. Kamiya,
536 and M. Seo. 2012. "Identification of an abscisic acid transporter by functional screening using the
537 receptor complex as a sensor." *Proceedings of the National Academy of Sciences of the United*
538 *States of America* 109, no. 24: 9653-9658. https://doi.org/10.1073/pnas.120356710.
539
540 Kiba, T., K. Takei, M. Kojima, and H. Sakakibara. 2013. "Side-chain modification of cytokinins
541 controls shoot growth in *Arabidopsis*." *Developmental Cell* 27, no. 4: 452–461.
542 https://doi.org/10.1016/j.devcel.2013.10.004.
543

544 Kiba, T., J. Inaba, T. Kudo, et al. 2018. "Repression of nitrogen starvation responses by members
545 of the Arabidopsis GARP-type transcription factor NIGT1/HRS1 subfamily." *The Plant Cell* 30,
546 no. 4: 925–945. https://doi.org/10.1105/tpc.17.00810.
547
548 Ko, D., J. Kang, T. Kiba, et al. 2014. "*Arabidopsis* ABCG14 is essential for the root-to-shoot
549 translocation of cytokinin." *Proceedings of the National Academy of Sciences of the United States*
550 *of America* 111, no. 19: 7150–7155. https://doi.org/10.1073/pnas.132151911.
551
552 Kobayashi, R., Y. Ohkubo, M. Izumi, et al. 2023. "Integration of shoot-derived polypeptide
553 signals by root TGA transcription factors is essential for survival under fluctuating nitrogen
554 environments." *Nature Communications* 15: 6903. https://doi.org/10.1038/s41467-024-51091-5.
555
556 Kojima, M., T. Kamada-Nobusada, H. Komatsu, et al. 2009. "Highly sensitive and high-
557 throughput analysis of plant hormones using MS-probe modification and liquid chromatography–
558 tandem mass spectrometry: an application for hormone profiling in *Oryza sativa*." *Plant and Cell*
559 *Physiology* 50, no. 7: 1201–1214. https://doi.org/10.1093/pcp/pcp057.
560
561 Krapp, A., R. Berthomé, M. Orsel, S. Mercey-Boutet, A. Yu, L. Castaings, S. Elftieh, H. Major,
562 J. P. Renou, and F. Daniel-Vedele. 2011. "Arabidopsis roots and shoots show distinct temporal
563 adaptation patterns toward nitrogen starvation." *Plant Physiology* 157, no. 3: 1255–1282.
564 https://doi.org/10.1104/pp.111.179838.
565
566 Krouk, G, B. Lacombe, A. Bielach, et al. 2010. "Nitrate-regulated auxin transport by NRT1.1
567 defines a mechanism for nutrient sensing in plants." *Developmental Cell* 18, no. 6: 927-937.
568 https://doi.org/10.1016/j.devcel.2010.05.008.
569

570 Langmead, B., C. Trapnell, M. Pop, and S. L. Salzberg. 2009. "Ultrafast and memory-efficient
571 alignment of short DNA sequences to the human genome." *Genome Biology* 10: R25.
572 https://doi.org/10.1186/gb-2009-10-3-r25.
573
574 Liu, K. H., C. Y. Huang, and Y. F. Tsay. 1999. "CHL1 is a dual-affinity nitrate transporter of
575 Arabidopsis involved in multiple phases of nitrate uptake." *The Plant Cell* 11, no. 5: 865–874.
576 https://doi.org/10.1105/tpc.11.5.865.
577
578 Liu, K. H., Y. Niu, M. Konishi, et al. 2017. "Discovery of nitrate–CPK–NLP signalling in central
579 nutrient–growth networks." *Nature* 545, no. 7654: 311–316. https://doi.org/10.1038/nature22077.
580
581 Liu, K. H., M. Liu, Z. Lin, Z. F. Wang, B. Chen, C. Liu, A. Guo, M. Konishi, S. Yanagisawa, and
582 J. Sheen. 2022. "NIN-like protein 7 transcription factor is a plant nitrate sensor." *Science* 377, no.
583 6613: 1419–1425. https://doi.org/10.1126/science.add1104.
584
585 Maeda, Y., M. Konishi, T. Kiba, Y. Sakuraba, N. Sawaki, T. Kurai, Y. Ueda, H. Sakakibara, and
586 S. Yanagisawa. 2018. "A NIGT1-centred transcriptional cascade regulates nitrate signalling and
587 incorporates phosphorus starvation signals in *Arabidopsis*." *Nature Communications* 9: 1376.
588 https://doi.org/10.1038/s41467-018-03832-6.
589
590 Medici, A., and G. Krouk. 2014. "The primary nitrate response: a multifaceted signalling
591 pathway." *Journal of Experimental Botany* 65, no. 19: 5567–5576.
592 https://doi.org/10.1093/jxb/eru245.
593
594 Miyawaki, K., M. Matsumoto-Kitano, and T. Kakimoto. 2004. "Expression of cytokinin
595 biosynthetic isopentenyltransferase genes in *Arabidopsis*: tissue specificity and regulation by

596 auxin, cytokinin, and nitrate." *The Plant Journal* 37, no. 1: 128–138.
597 https://doi.org/10.1046/j.1365-313X.2003.01945.x.
598
599 Miyawaki, K., P. Tarkowski , M. Matsumoto-Kitano, T. Kato, S. Sato, D. Tarkowska, S. Tabata,
600 G. Sandberg, and T. Kakimoto. 2006. "Roles of *Arabidopsis* ATP/ADP isopentenyltransferases
601 and tRNA isopentenyltransferases in cytokinin biosynthesis." *Proceedings of the National*
602 *Academy of Sciences of the United States of America* 103, no. 44: 16598–16603.
603 https://doi.org/10.1073/pnas.0603522103.
604
605 Monden, K., T. Kamiya, D. Sugiura, T. Suzuki, T. Nakagawa, and T. Hachiya. 2022. "Root-
606 specific activation of plasma membrane H^+-ATPase 1 enhances plant growth and shoot
607 accumulation of nutrient elements under nutrient-poor conditions in *Arabidopsis thaliana*."
608 *Biochemical and Biophysical Research Communications* 621, no. 17: 39–45.
609 https://doi.org/10.1016/j.bbrc.2022.06.097.
610
611 Ohkubo, Y., M. Tanaka, R. Tabata, M. Ogawa-Ohnishi, and Y. Matsubayashi. 2017. "Shoot-to-
612 root mobile polypeptides involved in systemic regulation of nitrogen acquisition." *Nature Plants*
613 3: 17029. https://doi.org/10.1038/nplants.2017.29.
614
615 Okamoto, Y., T. Suzuki, D. Sugiura, T. Kiba, H. Sakakibara, and T. Hachiya. 2019. "Shoot nitrate
616 underlies a perception of nitrogen satiety to trigger local and systemic signaling cascades in
617 *Arabidopsis thaliana*." *Soil Science and Plant Nutrition* 65, no. 1: 56–64.
618 https://doi.org/10.1080/00380768.2018.1537643.
619

620 Osugi, A., M. Kojima, Y. Takebayashi, N. Ueda, T. Kiba, and H. Sakakibara. 2017. "Systemic
621 transport of *trans*-zeatin and its precursor have differing roles in *Arabidopsis* shoots." *Nature*
622 *Plants* 3: 17112. https://doi.org/10.1038/nplants.2017.112.
623
624 Ota, R., Y. Ohkubo, Y. Yamashita, M. Ogawa-Ohnishi, and Y. Matsubayashi. 2020. "Shoot-to-
625 root mobile CEPD-like 2 integrates shoot nitrogen status to systemically regulate nitrate uptake
626 in *Arabidopsis*." *Nature Communications* 11: 641. https://doi.org/10.1038/s41467-020-14440-8.
627
628 Patterson, K., L. A. Walters, A. M. Cooper, J. G. Olvera, M. A. Rosas, A. G. Rasmusson, and M.
629 A. Escobar. 2016. "Nitrate-regulated glutaredoxins control Arabidopsis primary root growth."
630 *Plant Physiology* 170, no. 2: 989–999. https://doi.org/10.1104/pp.15.01776.
631
632 Poitout, A., A. Crabos, I. Petřík, O. Novák, G. Krouk, B. Lacombe, and S. Ruffel. 2018.
633 "Responses to systemic nitrogen signaling in Arabidopsis roots involve *trans*-zeatin in shoots."
634 *The Plant Cell* 30, no. 6: 1243–1257. https://doi.org/10.1105/tpc.18.00011.
635
636 Remans, T., P. Nacry, M. Pervent, S. Filleur, E. Diatloff, E. Mounier, P. Tillard, B. G. Forde, and
637 A. Gojon. 2006. "The *Arabidopsis* NRT1.1 transporter participates in the signaling pathway
638 triggering root colonization of nitrate-rich patches." *Proceedings of the National Academy of*
639 *Sciences of the United States of America* 103, no. 50: 19206–19211.
640 https://doi.org/10.1073/pnas.060527510.
641
642 Riveras, E., J. M. Alvarez, E. A. Vidal, C. Oses, A. Vega, and R. A. Gutiérrez. 2015. "The calcium
643 ion is a second messenger in the nitrate signaling pathway of Arabidopsis." *Plant Physiology* 169,
644 no. 2: 1397–1404. https://doi.org/10.1104/pp.15.00961.
645

646 Rubin, G., T. Tohge, F. Matsuda, K. Saito, and W. R. Scheible. 2009. "Members of the *LBD*
647 family of transcription factors repress anthocyanin synthesis and affect additional nitrogen
648 responses in *Arabidopsis*." *The Plant Cell* 21, no. 11: 3567–3584.
649 https://doi.org/10.1105/tpc.109.067041.
650
651 Ruffel, S., G. Krouk, D. Ristova, D. Shasha, K. D. Birnbaum, and G. M. Coruzzi. 2011. "Nitrogen
652 economics of root foraging: transitive closure of the nitrate–cytokinin relay and distinct systemic
653 signaling for N supply vs. demand." *Proceedings of the National Academy of Sciences of the*
654 *United States of America* 108, no. 45: 18524–18529. https://doi.org/10.1073/pnas.1108684108.
655
656 Sakakibara, H., K. Takei, and N. Hirose. 2006. "Interactions between nitrogen and cytokinin in
657 the regulation of metabolism and development." *Trends in Plant Science* 11, no. 9: 440–448.
658 https://doi.org/10.1016/j.tplants.2006.07.004.
659
660 Sakakibara, H. 2021. "Cytokinin biosynthesis and transport for systemic nitrogen signaling." The
661 *Plant Journal* 105, no. 2: 421–430. https://doi.org/10.1111/tpj.15011.
662
663 Safi, A., A. Medici, W. Szponarski, et al. 2021. "GARP transcription factors repress Arabidopsis
664 nitrogen starvation response via ROS-dependent and -independent pathways." *Journal of*
665 *Experimental Botany* 72, no. 10: 3881–3901. https://doi.org/10.3390/ijms22168685.
666
667 Scheible, W. R., M. Lauerer, E. D. Schulze, M. Caboche, and M. Stitt. 1997. "Accumulation of
668 nitrate in the shoot acts as a signal to regulate shoot-root allocation in tobacco." *The Plant Journal*
669 11, no. 4: 671–691. https://doi.org/10.1046/j.1365-313X.1997.11040671.x.
670

671 Signora, L., I. De Smet, C. H. Foyer, and H. Zhang. 2001. "ABA plays a central role in mediating
672 the regulatory effects of nitrate on root branching in *Arabidopsis*." *The Plant Journal* 28, no. 6:
673 655–662. https://doi.org/10.1046/j.1365-313x.2001.01185.x.
674
675 Takei, K., N. Ueda, K. Aoki, T. Kuromori, T. Hirayama, K. Shinozaki, T. Yamaya, and H.
676 Sakakibara. 2004a. "*AtIPT3* is a key determinant of nitrate-dependent cytokinin biosynthesis in
677 *Arabidopsis*." *Plant and Cell Physiology* 45, no. 8: 1053–1062.
678 https://doi.org/10.1093/pcp/pch119.
679
680 Takei, K., T. Yamaya, and H. Sakakibara. 2004b. "Arabidopsis *CYP735A1* and *CYP735A2*
681 encode cytokinin hydroxylases that catalyze the biosynthesis of *trans*-zeatin." *Journal of*
682 *Biological Chemistry* 279, no. 40: 41866–41872. https://doi.org/10.1074/jbc.M406337200.
683
684 Wang, R., R. Tischner, R. A. Gutiérrez, M. Hoffman, X. Xing, M. Chen, G. Coruzzi, and N. M.
685 Crawford. 2004. "Genomic analysis of the nitrate response using a nitrate reductase-null mutant
686 of Arabidopsis." *Plant Physiology* 136, no. 1: 2512–2522. https://doi.org/10.1104/pp.104.044610.
687
688 Wang, R, X. Xing, and N. M. Crawford. 2007. "Nitrite acts as a transcriptome signal at
689 micromolar concentrations in Arabidopsis roots." *Plant Physiology* 145, no. 4: 1735–1745.
690 https://doi.org/10.1104/pp.107.108944.
691
692 Wang, X., C. Feng, L. Tian, et al. 2021. "A transceptor–channel complex couples nitrate sensing
693 to calcium signaling in *Arabidopsis*." *Molecular Plant* 14, no. 5: 774–786.
694 https://doi.org/10.1016/j.molp.2021.02.005.
695

696 Zhou, Y., B. Zhou, L. Pache, M. Chang, A. H. Khodabakhshi, O. Tanaseichuk, C. Benner, and S.
697 K. Chanda. 2019. "Metascape provides a biologist-oriented resource for the analysis of systems-
698 level datasets." *Nature Communications* 10: 1523. https://doi.org/10.1038/s41467-019-09234-6.
699
700 Zhang, H., A. Jennings, P. W. Barlow, and B. G. Forde. 1999. "Dual pathways for regulation of
701 root branching by nitrate." *Proceedings of the National Academy of Sciences of the United States*
702 *of America* 96, no. 11: 6529–6534. https://doi.org/10.1073/pnas.96.11.6529.
703
704 Zhang, K., O. Novak, Z. Wei, M. Gou, X. Zhang, Y. Yu, H. Yang, Y. Cai, M. Strnad, and C. J.
705 Liu. 2014. "*Arabidopsis* ABCG14 protein controls the acropetal translocation of root-synthesized
706 cytokinins." *Nature Communications* 5: 3274. https://doi.org/10.1038/ncomms4274.
707
708 **Supporting Information**
709 Additional supporting information can be found online in the Supporting Information section.
710
711 **Figure Legends**
712 **Figure 1.** Micrografting and transfer experiments for manipulation of nitrate levels and *IPT3*
713 expression in a shoot-specific manner. (A) Summary of the micrografting and transfer
714 experiments. (B, C) Nitrate concentrations in shoots (B) and roots (C) 0, 3, or 5 days after nitrogen
715 removal. (D, E) Total protein concentrations in shoots (D) and roots (E) 5 days after nitrogen
716 removal. (B–E) Two grafted plants were pooled as one biological replicate. Data are presented as
717 mean ± SD (n = 3). (F, G) Total nitrogen concentrations in shoots (F) and roots (G) 5 days after
718 nitrogen removal. Sampling was performed three times independently. In this sampling, 7, 6, and
719 5 grafted plants were pooled as one biological replicate. Data are presented as mean ± SD (n = 3).
720 (B–G) Different lowercase letters indicate significant differences, as determined via Tukey–
721 Kramer test ($P < 0.05$). (H) Transcript levels of *IPT3* in shoots 5 days after nitrogen removal, as

722 determined using RT-qPCR. Sampling was done five times independently. In this sampling, 9, 6,
723 7, 7, and 8 grafted plants were pooled as one biological replicate. Data are presented as mean ±
724 SD (n = 5). (I) Nitrate concentrations in shoots 5 days after nitrogen removal. (J) Transcript levels
725 of *GFP* in shoots 5 days after nitrogen removal, as determined via RT-qPCR. (I, J) One biological
726 replicate consisted of one grafted plant. Data are presented as mean ± SD (n = 3). (H–J) Statistical
727 significance was assessed using unpaired two-tailed Welch's *t*-test (*$P < 0.05$; **$P < 0.01$;
728 ***$P < 0.001$). (K) Fluorescence images of true leaves 5 days after nitrogen removal. Green and
729 red colors correspond to GFP fluorescence and autofluorescence, respectively. Scale bars
730 represent 500 μm. (B–K) In graph legends, the grafted plants are indicated as "scion line
731 name/rootstock line name." ns, not significant; FW, fresh weight; DW, dry weight.
732
733 **Figure 2.** Effects of shoot nitrate status and shoot *IPT3* expression on the shoot and root
734 concentrations of CK species. (A–M) The shoot and root concentrations of iP (A), iPR (B), iPRPs
735 (C), iP7G (D), iP9G (E), *t*Z (F), *t*ZR (G), *t*ZPRs (H), *t*Z7G (I), *t*Z9G (J), *t*ZOG (K), *t*ZROG (L),
736 and *t*ZRPsOG (M) in the grafted plants 5 days after nitrogen removal. Sampling was performed
737 three times independently. In the sampling, 7, 6, and 5 grafted plants were pooled as one
738 biological replicate. Data are presented as mean ± SD [n = 3, excluding iP concentrations in
739 Col/*ipt3,5,7* roots and *ipt3*/*ipt3,5,7* roots (n = 2)]. Different lowercase letters indicate significant
740 differences, as determined via Tukey–Kramer test ($P < 0.05$). Regarding the shoot concentrations
741 of iP and *t*ZRPsOG, unpaired two-tailed Welch's *t*-test was run at $\alpha = 0.05$. iP, N^6-(Δ^2-
742 isopentenyl)adenine; iPR, iP riboside; iPRPs, iP ribotides; iP7G, iP-7-*N*-glucoside; iP9G, iP-9-*N*-
743 glucoside; *t*Z, *trans*-zeatin; *t*ZR, *t*Z riboside; *t*ZRPs, *t*Z ribotides; *t*Z7G, *t*Z-7-*N*-glucoside; *t*Z9G,
744 *t*Z-9-*N*-glucoside; *t*ZOG, *t*Z-*O*-glucoside; *t*ZROG, *t*ZR-*O*-glucoside; *t*ZRPsOG, *t*ZRPs-*O*-
745 glucoside; ns, not significant; nd, not detected; FW, fresh weight.
746

747 **Figure 3.** Effects of shoot nitrate status and shoot *IPT3* expression on plant growth. (A)
748 Representative shoot appearance of grafted plants. Scale bars represent 5 mm. (B–F) Shoot fresh
749 weight (B), leaf blade area (C), rosette diameter (D), leaf number (E), and root fresh weights (F)
750 of grafted plants 5 days after nitrogen removal. All data pooled from five independent grafting
751 experiments are presented as mean ± SD (n = 33). Different lowercase letters indicate significant
752 differences, as determined via Tukey–Kramer test ($P < 0.05$). ns, not significant; FW, fresh weight.
753
754 **Figure 4.** Effects of shoot nitrate status and shoot *IPT3* expression on the shoot and root
755 transcriptomes. RNA-seq was performed using the shoots and roots of grafted plants 5 days after
756 nitrogen removal. Sampling was performed three times independently. In the sampling, 9, 6, and
757 7 grafted plants were pooled as one biological replicate. (A) Venn diagram presenting the number
758 of DEGs at a minimum fold change of 1.5 in NR-null/*ipt3,5,7* plants relative to Col/*ipt3,5,7* plants
759 and in NR-null *ipt3*/*ipt3,5,7* plants relative to *ipt3*/*ipt3,5,7* plants. (B–E) Plots of normalized
760 transcript levels of 631 DEGs (B) and 663 DEGs (C) in shoots and 189 DEGs (D) and 126 DEGs
761 (E) in roots. 1st, 2nd, and 3rd denote the order of three independent experiments. Different
762 lowercase letters indicate significant differences, as determined via Tukey–Kramer test ($P < 0.05$).
763 The numbers on the graph represent the difference in mean values.
764
765 **Figure 5.** Effects of shoot nitrate status and shoot *IPT3* expression on nitrogen-related
766 transcriptional responses in shoots and roots. (A–D) Plots of mean normalized transcript levels of
767 nitrate (*per se*)-inducible genes in 2 h (A), genes induced via CPK10/30/32 (B), genes commonly
768 induced via all NLPs (C), and nitrogen starvation-inducible genes (D) in the shoots and roots of
769 grafted plants 5 days after nitrogen removal. The gene lists were obtained from Wang et al. (2004)
770 for (A), Liu et al. (2017) for (B), Liu et al. (2022) for (C), and Kiba et al. (2018) and Krapp et al.
771 (2011) for (D). Different lowercase letters indicate significant differences, as determined via
772 Tukey–Kramer test ($P < 0.05$). The numbers on the graph represent the difference in mean values.

773 (E–G) Transcriptional changes in genes involved in nitrogen transport and assimilation in roots
774 (E), genes encoding transcription factors for nitrogen starvation responses in shoots (F) and in
775 roots (G), and genes encoding shoot-to-root mobile peptides in shoots (H) in grafted plants 5 days
776 after nitrogen removal. The normalized transcript levels were visualized as heatmaps using
777 MORPHEUS (https://software.broadinstitute.org/morpheus). The relative color scheme uses the
778 minimum (blue) and maximum (yellow) values in each row. 1st, 2nd, and 3rd denote the order of
779 three independent experiments. ns, not significant; TF, transcription factor.
780
781 **Figure 6.** Summary of systemic responses to shoot nitrate satiety and their dependence by shoot
782 IPT3.

Figure 1

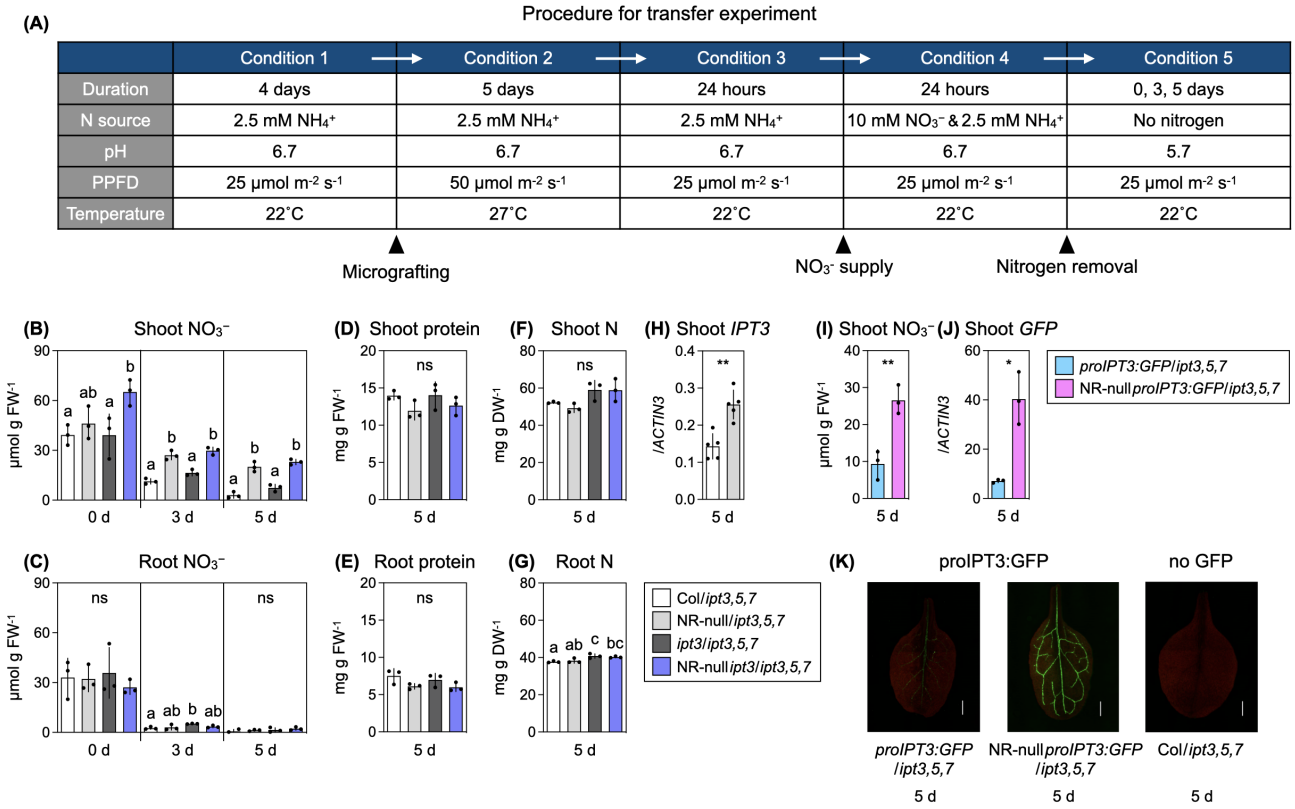

Figure 1. Micrografting and transfer experiments for manipulation of nitrate levels and *IPT3* expression in a shoot-specific manner. (A) Summary of the micrografting and transfer experiments. (B, C) Nitrate concentrations in shoots (B) and roots (C) 0, 3, or 5 days after nitrogen removal. (D, E) Total protein concentrations in shoots (D) and roots (E) 5 days after nitrogen removal. (B–E) Two grafted plants were pooled as one biological replicate. Data are presented as mean ± SD (n = 3). (F, G) Total nitrogen concentrations in shoots (F) and roots (G) 5 days after nitrogen removal. Sampling was performed three times independently. In this sampling, 7, 6, and 5 grafted plants were pooled as one biological replicate. Data are presented as mean ± SD (n = 3). (B–G) Different lowercase letters indicate significant differences, as determined via Tukey–Kramer test ($P < 0.05$). (H) Transcript levels of *IPT3* in shoots 5 days after nitrogen removal, as determined using RT-qPCR. Sampling was done five times independently. In this sampling, 9, 6, 7, 7, and 8 grafted plants were pooled as one biological replicate. Data are presented as mean ± SD (n = 5). (I) Nitrate concentrations in shoots 5 days after nitrogen removal. (J) Transcript levels of *GFP* in shoots 5 days after nitrogen removal, as determined via RT-qPCR. (I, J) One biological replicate consisted of one grafted plant. Data are presented as mean ± SD (n = 3). (H–J) Statistical significance was assessed using unpaired two-tailed Welch's *t*-test (*$P < 0.05$; **$P < 0.01$; ***$P < 0.001$). (K) Fluorescence images of true leaves 5 days after nitrogen removal. Green and red colors correspond to GFP fluorescence and autofluorescence, respectively. Scale bars represent 500 μm. (B–K) In graph legends, the grafted plants are indicated as "scion line name/rootstock line name." ns, not significant; FW, fresh weight; DW, dry weight.

Figure 2

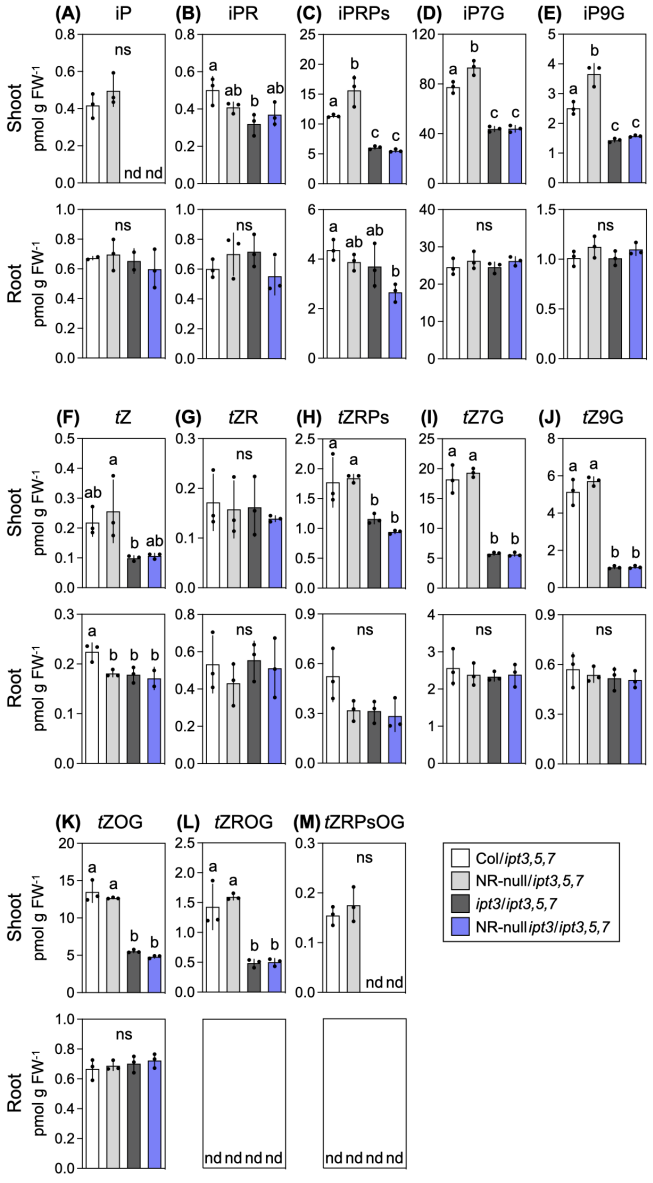

Figure 2. Effects of the shoot nitrate status and shoot *IPT3* expression on the shoot and root concentrations of CK species. (A–M) The shoot and root concentrations of iP (A), iPR (B), iPRPs (C), iP7G (D), iP9G (E), *t*Z (F), *t*ZR (G), *t*ZPRs (H), *t*Z7G (I), *t*Z9G (J), *t*ZOG (K), *t*ZROG (L), and *t*ZRPsOG (M) in the grafted plants 5 days after nitrogen removal. Sampling was performed three times independently. In the sampling, 7, 6, and 5 grafted plants were pooled as one biological replicate. Data are presented as mean ± SD [n = 3, excluding iP concentrations in Col/*ipt3,5,7* roots and *ipt3*/*ipt3,5,7* roots (n = 2)]. Different lowercase letters indicate significant differences, as determined via Tukey–Kramer test ($P < 0.05$). Regarding the shoot concentrations of iP and *t*ZRPsOG, unpaired two-tailed Welch's *t*-test was run at $\alpha = 0.05$. iP, N^6-(Δ^2-isopentenyl)adenine; iPR, iP riboside; iPRPs, iP ribotides; iP7G, iP-7-*N*-glucoside; iP9G, iP-9-*N*-glucoside; *t*Z, *trans*-zeatin; *t*ZR, *t*Z riboside; *t*ZRPs, *t*Z ribotides; *t*Z7G, *t*Z-7-*N*-glucoside; *t*Z9G, *t*Z-9-*N*-glucoside; *t*ZOG, *t*Z-*O*-glucoside; *t*ZROG, *t*ZR-*O*-glucoside; *t*ZRPsOG, *t*ZRPs-*O*-glucoside; ns, not significant; nd, not detected; FW, fresh weight.

Figure 3

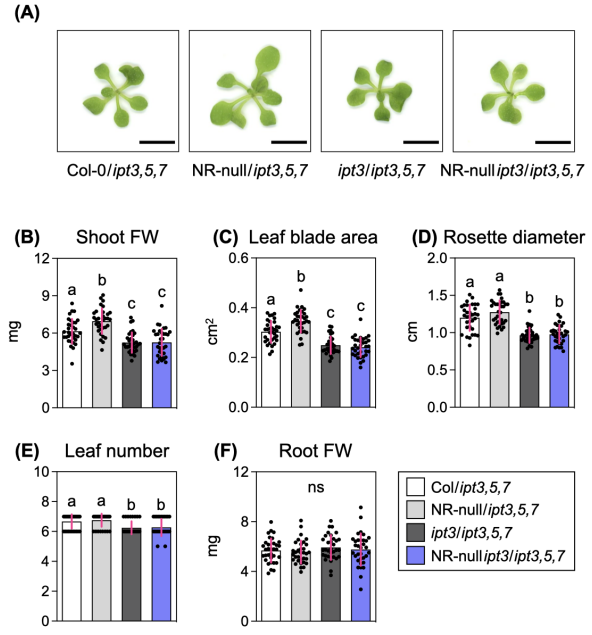

Figure 3. Effects of the shoot nitrate status and shoot *IPT3* expression on plant growth. (A) Representative shoot appearance of grafted plants. Scale bars represent 5 mm. (B–F) Shoot fresh weights (B), leaf blade area (C), rosette diameter (D), leaf number (E), and root fresh weights (F) of grafted plants 5 days after nitrogen removal. All data pooled from five independent grafting experiments are presented as mean ± SD (n = 33). Different lowercase letters indicate significant differences, as determined via Tukey–Kramer test ($P < 0.05$). ns, not significant; FW, fresh weight.

Figure 4

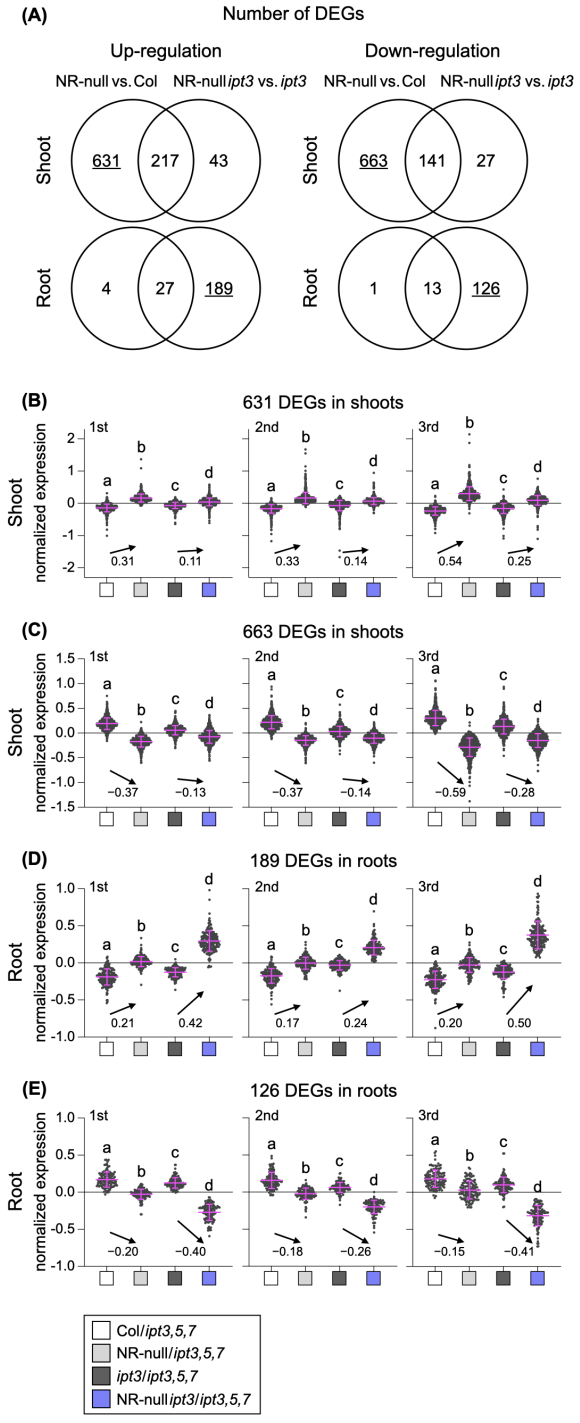

Figure 4. Effects of the shoot nitrate status and shoot *IPT3* expression on the shoot and root transcriptomes. RNA-seq was performed using the shoots and roots of grafted plants 5 days after nitrogen removal. Sampling was performed three times independently. In the sampling, 9, 6, and 7 grafted plants were pooled as one biological replicate. (A) Venn diagram presenting the number of DEGs at a minimum fold change of 1.5 in NR-null/*ipt3,5,7* plants relative to Col/*ipt3,5,7* plants and in NR-null *ipt3*/*ipt3,5,7* plants relative to *ipt3*/*ipt3,5,7* plants. (B–E) Plots of normalized transcript levels of 631 DEGs (B) and 663 DEGs (C) in shoots and 189 DEGs (D) and 126 DEGs (E) in roots. 1st, 2nd, and 3rd denote the order of three independent experiments. Different lowercase letters indicate significant differences, as determined via Tukey–Kramer test ($P < 0.05$). The numbers on the graph represent the difference in mean values.

Figure 5

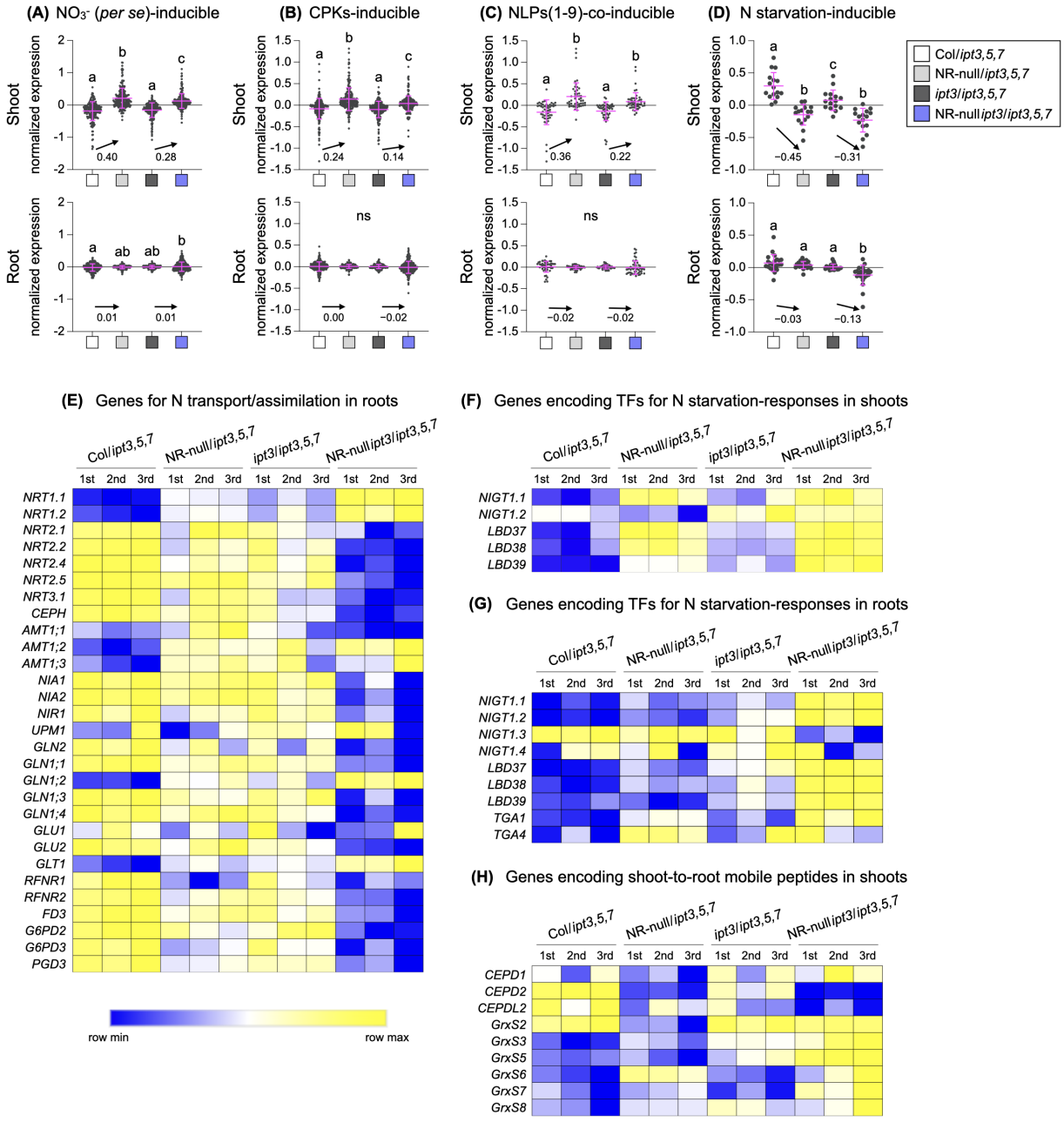

Figure 5. Effects of the shoot nitrate status and shoot *IPT3* expression on nitrogen-related transcriptional responses in shoots and roots. (A–D) Plots of mean normalized transcript levels of nitrate (*per se*)-inducible genes in 2 h (A), genes induced via CPK10/30/32 (B), genes commonly induced via all NLPs (C), and nitrogen starvation-inducible genes (D) in the shoots and roots of grafted plants 5 days after nitrogen removal. The gene lists were obtained from Wang et al. (2004) for (A), Liu et al. (2017) for (B), Liu et al. (2022) for (C), and Kiba et al. (2018) and Krapp et al. (2011) for (D). Different lowercase letters indicate significant differences, as determined via Tukey–Kramer test ($P < 0.05$). The numbers on the graph represent the difference in mean values. (E–G) Transcriptional changes in genes involved in nitrogen transport and assimilation in roots (E), genes encoding transcription factors for nitrogen starvation responses in shoots (F) and in roots (G), and genes encoding shoot-to-root mobile peptides in shoots (H) in grafted plants 5 days after nitrogen removal. The normalized transcript levels were visualized as heatmaps using MORPHEUS (https://software.broadinstitute.org/morpheus). The relative color scheme uses the minimum (blue) and maximum (yellow) values in each row. 1st, 2nd, and 3rd denote the order of three independent experiments. ns, not significant; TF, transcription factor.

Figure 6

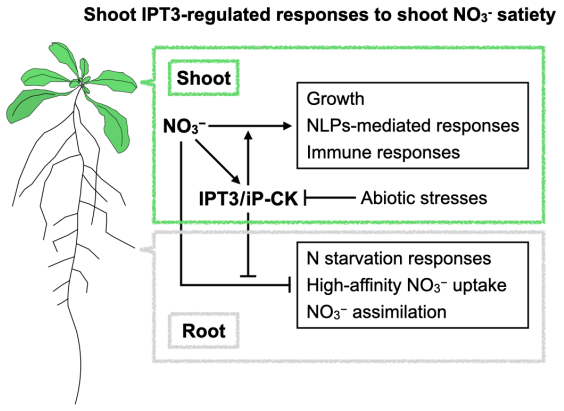

Figure 6. Summary of systemic responses to shoot nitrate satiety and their modulation by shoot IPT3.